

ADAPTIVE CONTROL OF NETWORKS OF DELAY-COUPLED CHAOTIC SYSTEMS

P. Yu. Guzenko

High Mathematics Department
SPb State Polytechnical University,
Russia

J. Lehnert

Institut für Theoretische Physik
Technische Universität Berlin
Germany

A. L. Fradkov

Department of Theoretical Cybernetics
Saint-Petersburg State University
Saint-Petersburg
Russia

E. Schöll

Institut für Theoretische Physik
Technische Universität Berlin
Germany

Abstract

We show that in delay-coupled networks of chaotic Rössler systems local stabilization of unstable periodic orbits and global synchronization of these orbits is simultaneously possible. Based on the well-know speed gradient method of control theory, we derive an adaptation algorithm to tune the feedback gain and the coupling strength. Our simulations show that this algorithm finds appropriate values for achieving stabilization and synchronization in small ring networks. Even in the case of disturbance by noise the algorithm can be successfully applied.

Key words

synchronization, stabilization, chaos, adaptive control, networks

1 Introduction

Over the past decades the control of nonlinear dynamical systems has evolved into a wide interdisciplinary area of research [Schöll, Schuster, 2007]. This field has various aspects comprising stabilization of unstable periodic orbits embedded in a deterministic chaotic attractor, which is generally referred to as *chaos control*, stabilization of unstable fixed points (steady states), or control of the coherence and timescales of stochastic motion. One scheme where the control force is constructed from time-delayed signals [Pyragas, 1992] has turned out to be very robust and universal to apply, and easy to implement experimentally. It has been used in a large variety of systems in physics, chemistry, biology, medicine, and engineering [Pyragas, 2006; Schöll, Schuster, 2007], in purely temporal dynamics as well as in spatially extended systems [Kim et.al.,2001; Baba et.al.,2002; Schlesner et.al.,2003; Postlethwaite and Silber,2007;

Ahlborn and Parlitz,2008; Kehrt et.al.,2009; Kyrychko et.al.,2009]. In time-delayed feedback control (*time-delay autosynchronization*) the control signal is built from the difference $s(t) - s(t - \tau)$ between the present and an earlier value of an appropriate system variable s . It is *non-invasive* since the control forces vanish if the target state (a periodic state of period τ or a steady state) is reached. Thus the unstable states themselves of the uncontrolled system are not changed, but only their neighbourhood is adjusted such that neighbouring trajectories converge to it, *i.e.*, the control forces act only if the system deviates from the state to be stabilized. Involving no numerically expensive computations, time-delayed feedback control is capable of controlling systems with very fast dynamics still in real-time mode, and detailed knowledge of the target state is not required.

Moreover, control of dynamics on delay-coupled networks has recently gained much interest. Synchronization phenomena in networks are of great importance [Pikovsky et.al.,2001] in many areas ranging from physics and chemistry to biology and engineering. In general, the stability depends in a complicated way on the local dynamics of the nodes and the coupling topology. In-phase (zero-lag) synchronization as well as various cluster synchronization states, where certain clusters inside the network show isochronous synchronization, can be realized by tuning the coupling parameters such as the coupling phase, coupling strength, and delay time [Choe et.al.,2009; Dahms et.al., 2012].

To find appropriate values of these control parameters, the speed-gradient method [Fradkov, 1979; Fradkov, 2005; Fradkov, 2007] from control theory can be applied to stabilize a desired unstable state [Guzenko et.al., 2008; Lehnert et.al., 2011] or to achieve a desired state of generalized synchrony (*adaptive synchronization*) in a network of periodic Stuart-Landau oscil-

lators [Selivanov et.al.,2012; Schöll et.al.,2012]. Here we apply the speed-gradient method to a delay-coupled network of chaotic Rössler systems to find appropriate values of the delayed feedback strength and the coupling constant to suppress chaos and stabilize unstable periodic states.

2 Stabilization and synchronization of periodic orbits in small networks of Rössler systems

2.1 Control of a single Rössler system

In this Section, we discuss the control of a single uncoupled Rössler system with time-delayed feedback control [Pyragas, 1992; Balanov et.al., 2005]. We use the Rössler model since it can be considered as paradigmatic for chaotic system. Without control, it exhibits chaotic oscillations born via a cascade of period-doubling bifurcations. The system with delayed feedback reads:

$$\begin{aligned} \dot{x} &= -y - z - K[x(t) - x(t - \tau)] \\ \dot{y} &= x + ay \\ \dot{z} &= b + z(x - \mu) \end{aligned} \quad (1)$$

where K is the self-feedback coefficient and τ is the delay time. We consider the system at the parameter values $a = 0.2$, $b = 0.2$, $\mu = 6.5$. All quantities used in this paper are dimensionless. For $K = 0$ and these parameters, Eq. (1) exhibits a chaotic attractor, as depicted in the top panel of Fig. 1. The unstable periodic orbits (UPO) embedded in this chaotic attractor can be stabilized with the appropriate choice of K and τ , where τ has to be equal to the period of the UPO to be stabilized. For instance, unstable periodic orbits with periods $T_1 \approx 5.91679$ ("period-1 orbit", see Fig. 1 bottom) and $T_2 \approx 11.82814$ ("period-2 orbit") exist and can be stabilized. In Ref. [Just et.al., 1997] it has been analytically predicted by a linear expansion that the control is successful only in a finite range of K values: at the lower control boundary the limit cycle undergoes a period-doubling bifurcation, and at the upper boundary a Hopf bifurcation generating a stable or an unstable torus from a limit cycle (Neimark-Sacker bifurcation). For instance, application of the delayed feedback with $\tau = T_1$ and $0.24 < K < 2.3$ stabilizes the period-1 orbit.

In the following, we will assume that the value of τ is known and appropriately chosen. Following previous work [Guzenko et.al., 2008; Lehnert et.al., 2011], we use the speed gradient (SG) method to find an adaptation algorithm for K (with zero initial condition). The speed-gradient method is a well known adaptive control technique which minimizes a predefined goal function by changing an accessible system parameter appropriately. The adaptation of the feedback gain may be useful for systems with unknown or slowly changing parameters as in these cases an analytical calculation of an appropriate value of K is not possible.

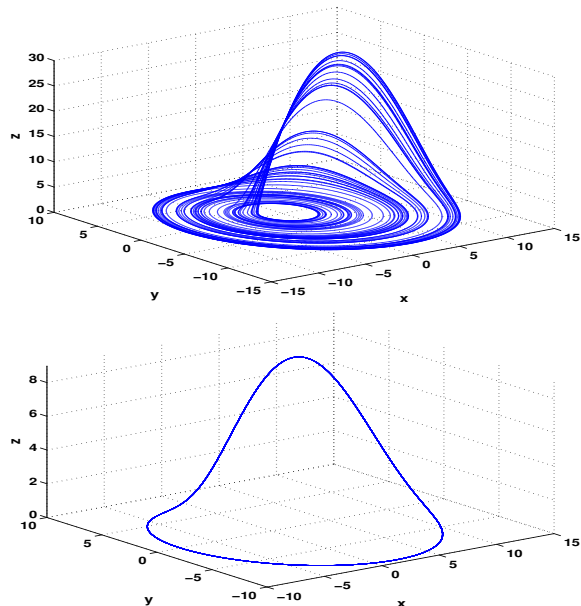


Figure 1. Chaotic attractor (top) and stabilized period-1 orbit (bottom) for the uncoupled Rössler system (Eq. (1)). System parameters: $a = 0.2$, $b = 0.2$, $\mu = 6.5$. Feedback control with $\tau \approx 5.91679$ is used in the bottom panel.

To obtain a speed-gradient adaptation algorithm for the feedback gain K let us choose the goal function as follows: $Q(x) = \frac{1}{2}(x(t) - x(t - \tau))^2$. The SG-algorithm in the differential form is given by $\dot{K} = -\gamma \nabla_K Q$, where $\gamma > 0$ is the adaptation gain. In the case of successful control, the SG-algorithm ensures $Q(x(t)) \rightarrow 0$ for $t \rightarrow +\infty$.

For system (1), we obtain:

$$\begin{aligned} \dot{Q} &= (x(t) - x(t - \tau))(\dot{x}(t) - \dot{x}(t - \tau)), \\ \dot{x}(t) &= -y(t) - z(t) - K[x(t) - x(t - \tau)] \\ \dot{x}(t - \tau) &= -y(t - \tau) - z(t - \tau) - \\ &\quad - K[x(t - \tau) - x(t - 2\tau)] \end{aligned} \quad (2)$$

$$\dot{K} = \gamma(x(t) - x(t - \tau))[x(t) - 2x(t - \tau) + x(t - 2\tau)] \quad (3)$$

Previous studies [Guzenko et.al., 2008; Lehnert et.al., 2011] show that this adaptation algorithm converges to some appropriate value of K stabilizing the period-1 orbit. In the following, we will investigate whether the adaptation of K can be used to suppress chaos not only in a single uncoupled node but also in delay-coupled networks of chaotic Rössler systems.

2.2 Networks of Rössler systems

Next, we consider a network of delay-coupled chaotic Rössler oscillators and apply local time-delayed feedback control with feedback strength K_j to each node j . Let N be the number of nodes and let $A = (a_{jk})$ be the coupling matrix. We set $a_{jj} = 0$ and assume a constant row sum equal to unity, i.e., $\sum_k a_{jk} = 1$ for $k = 1, \dots, N$. The dynamics is given by ($j = 1, \dots, N$):

$$\begin{aligned}
\dot{x}_j &= -y_j - z_j - K_j[x_j(t) - x_j(t - \tau)] + \\
&+ c \sum_{k=1}^N a_{jk}[x_k(t - \tau) - x_j(t)] \\
\dot{y}_j &= x_j + ay_j \\
\dot{z}_j &= b + z_j(x_j - \mu),
\end{aligned} \tag{4}$$

where c is the overall coupling strength.

Each node in the network has its own adaptation algorithm for K_j (with zero initial condition $K_j(0) = 0$):

$$\begin{aligned}
\dot{K}_j &= \gamma(x_j(t) - x_j(t - \tau))[x_j(t) - \\
&- 2x_j(t - \tau) + x_j(t - 2\tau)]
\end{aligned} \tag{5}$$

In the following we will focus on unidirectional rings, i.e, the coupling matrix is given by

$$A = \begin{pmatrix} 0 & 1 & 0 & \dots & 0 \\ 0 & 0 & 1 & \dots & 0 \\ \vdots & \vdots & \vdots & \ddots & \vdots \\ 0 & 0 & 0 & \dots & 1 \\ 1 & 0 & 0 & \dots & 0 \end{pmatrix}$$

We proceed as follows: In Section 2.3 we discuss the adaptation of K in small ring networks with the goal to stabilize the period-1 orbit. We investigate the range of the coupling constant c for which not only stabilization but also synchronization occurs. Section 2.4 extends our method by an additional adaptation algorithm for c . In Section 2.5, we present a slight modification of our algorithm which improves synchronization in cases where the period of the UPO is not exactly known. Furthermore, we conduct a linear stability analysis for this case. Finally, in Section 3 we modify our method in order to deal with noisy measurement.

2.3 Adaptation of the self-feedback in small ring networks

First we consider the smallest unidirectional ring network: a ring composed of 2 nodes. Figure 2 shows the successful adaptation of the two self-feedback coefficients K_1 and K_2 according to Eq. (5). If the control goal is reached, the adaptation of K stops. This follows from Eq. (5): $\dot{K}_j = 0$ for $x_j(t) = x_j(t - \tau)$; this shows up in Fig. 2 for $t > 500$. The fact that K_1 and K_2 approach different values is due to different initial conditions for node 1 and 2.

Computer simulations show that for different initial conditions $x_1(0) = 2$, $y_1(0) = \pm 2$, $x_2(0) = \pm 2$, $y_2(0) = \pm 2$, (4 combinations for two nodes, $z_1 = z_2 = 0$ always) and $\gamma = 0.05, 0.07$, the two nodes synchronize in the following range of c : $c \in [0.2, 0.8]$ (for $c = 0.9$ the system diverges). We define the maximal synchronization error in x as $\epsilon_x \equiv \max_{i,t > t_c} |x_i(t) - x_{(i+1) \bmod N}(t)|$, $i = 0, \dots, N$ where t_c is a sufficiently large time when convergence is reached. Analogously we define ϵ_y and ϵ_z . We assume the network

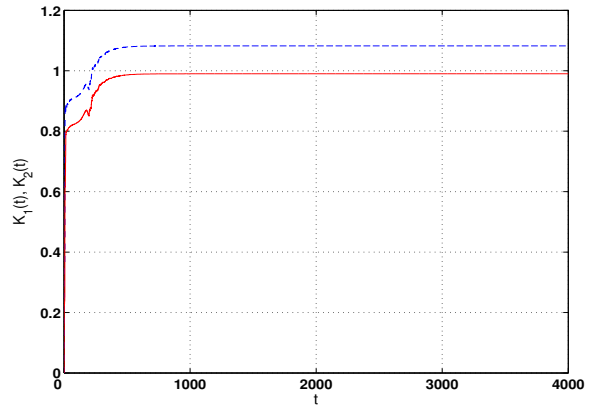


Figure 2. (Color online) $K_1(t)$ (red solid), $K_2(t)$ (blue dashed) adapted according to Eq. (4,5) for a 2-node network with $(x_0, y_0) = (2, 2)$ and $(2, -2)$; $z_0 = 0$. System parameters: $a = 0.2$, $b = 0.2$, $\mu = 6.5$, $\tau \approx 5.91679$, $\gamma = 0.05$.

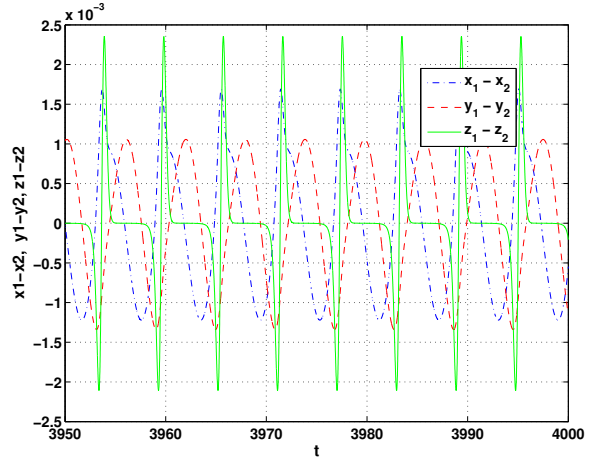


Figure 3. (Color online) Differences $x_1 - x_2$ (blue dash-dotted), $y_1 - y_2$ (red dashed) and $z_1 - z_2$ (green solid) vs time t adapted according to Eqs. (4) and (5). System parameters as in Fig. 2.

as synchronized if $\epsilon_x, \epsilon_y, \epsilon_z < 0.02$, which is very roughly 100 times less than the corresponding differences without coupling. Note that for the period-1 orbit the following estimates hold: $x(t) \in [-8; 10.5]$, $y(t) \in [-9.5; 6.9]$, $z(t) \in [0.014; 8.6]$. Figure 3 shows the synchronization error for $N = 2$. As can be seen, synchronization in the above sense is reached.

Perfect synchronization is not reached because in numerical simulations it is usually not possible, due to the finite integration step, to choose the time delay exactly equal to the period of the system. If $\tau = T + \delta$, where δ is some small positive or negative quantity, the local control of the i -th node, i.e., the term $K_i(x_i(t) - x_i(t - \tau))$, does not vanish completely if the UPO with period T is stabilized. Because the K_i have different values after adaptation, a slightly different orbit is induced in every node and perfect synchronization is not possible.

Now we investigate the persisting synchronization er-

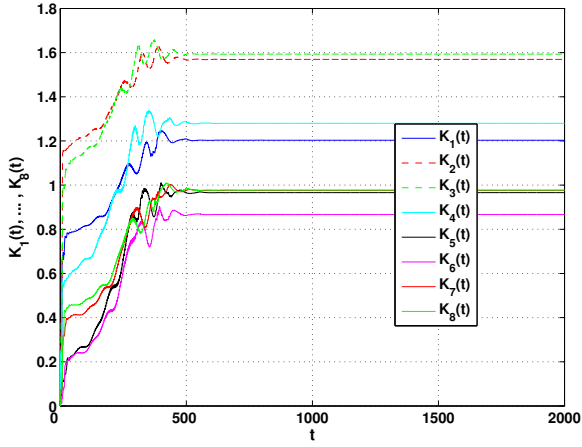


Figure 4. (Color online) Self-feedback coefficients $K_1(t), \dots, K_8(t)$ adapted according to Eqs. (4) and (5) for 8 nodes coupled in a unidirectional ring. System parameters as in Fig. 2.

ror for networks with $N = 4$ nodes. Computer simulations (not shown here) yield that for different initial conditions and $\gamma = 0.05, c = 0.3, 0.7, 0.8$ the nodes are synchronized in the sense discussed above (for $c = 0.3$ with $\varepsilon_x=0.03, \varepsilon_y=0.02, \varepsilon_z=0.04$; for $c = 0.7$ with $\varepsilon_x=0.009, \varepsilon_y=0.007, \varepsilon_z=0.012$; for $c = 0.8$ with $\varepsilon_x=0.007, \varepsilon_y=0.005$ and $\varepsilon_z=0.010$). Thus increasing the coupling coefficient inside the convergence range leads to increase of the accuracy of synchronization.

Next, we test our algorithm for larger networks of $N = 5, 8, 12, 13$ and 16 nodes. For 5 to 13 nodes, combinations of γ and c exist for which successful synchronization is possible. For a unidirectional ring of 16 nodes all attempts to find appropriate values of γ and c to synchronize the network failed although local stabilization still was achieved. In general, with an increasing number of nodes, the values of γ and c decrease as well as the range of these parameters suitable for control.

As an example for the control of a network with $N > 2$, we present the control of a network with 8 nodes. Figure 4 shows the time series for the self-feedback coefficients $K_1(t), \dots, K_8(t)$ and Fig. 5 shows the final synchronization accuracy (8 differences between y -coordinates). For $\gamma = 0.05, c = 0.3, 0.7$ our nodes are synchronized in the sense discussed above, and $\varepsilon_x=0.015, \varepsilon_y=0.013, \varepsilon_z=0.024$. For a unidirectional ring network composed of 12 nodes similar results were obtained.

For a unidirectional ring network composed of 13 nodes, it was found that for $\gamma = 0.025$ and $c = 0.25 \dots 0.95$ the nodes are synchronized in the sense discussed above (as well as for $\gamma = 0.02$), but for $c = 1.2$ the system diverges. For $\gamma = 0.03$ there are no appropriate values for c . For $\gamma = 0.01$ the period-1 orbit is stabilized in all nodes, but synchronization with appropriate accuracy is not found. Synchronization in a ring of 13 nodes was achieved with the following accuracy:

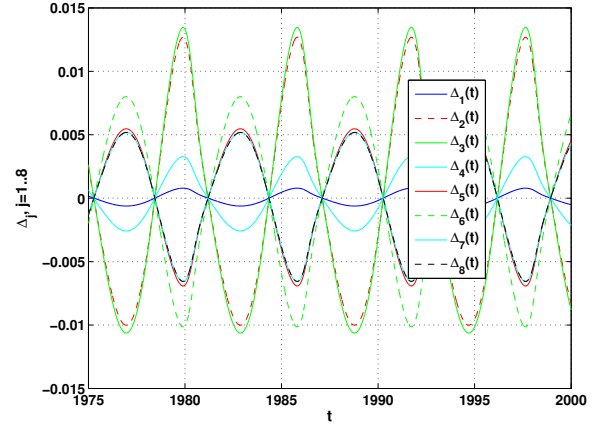


Figure 5. (Color online) Differences $\Delta_j = y_{(j+1)} - y_j, j = 1, \dots, 7, \Delta_8 = y_1 - y_8$ vs time t adapted according to Eqs. (4) and (5) for 8 nodes coupled in a unidirectional ring. $\gamma = 0.025$. Other parameters as in Fig. 2.

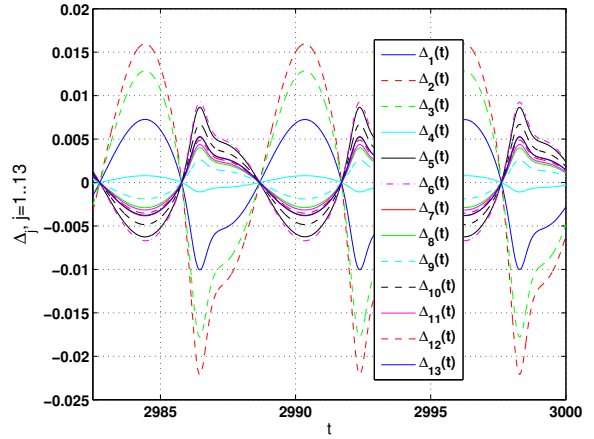


Figure 6. (Color online) Differences $\Delta_j = x_{j+1} - x_j, j = 1, \dots, 12, \Delta_{13} = y_1 - y_{13}$ vs time t adapted according to Eqs. (4) and (5) for 13 nodes coupled in a unidirectional ring. System parameters as in Fig. 2.

$\varepsilon_x=0.023, \varepsilon_y=0.017, \varepsilon_z=0.03$ (see Fig.6).

2.4 Adaption of self-feedback coefficients and coupling strength

As discussed in the previous Section, synchronization and stabilization is only feasible if the coupling coefficient c is chosen appropriately. In this Section, we show that it is possible to obtain the appropriate value of c by adapting c in addition to adapting K_1, \dots, K_N .

To obtain a speed-gradient adaptation algorithm for the coupling coefficient c , we choose a goal function based on the state of two nodes as follows: $Q_c(x) = \frac{1}{2}(x_1(t) - x_2(t - \tau))^2$. According to the SG-method, i.e., $\dot{K}_j = -\gamma_c \nabla_c \dot{Q}_{K_j}$ and $\dot{c} = -\gamma_c \nabla_c \dot{Q}_c$ we obtain for the simultaneous adaptation of K_1, \dots, K_N and c in

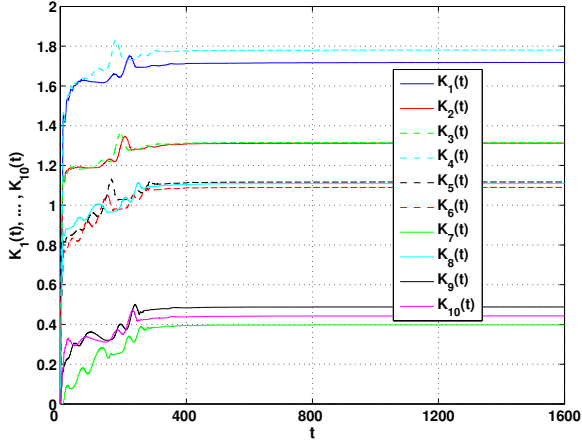


Figure 7. (Color online) Self-feedback coefficients $K_1(t), \dots, K_{10}(t)$ vs time t for 10-nodes coupled in a unidirectional ring. Adaptation algorithm according to Eq. (6). $\gamma = 0.015$, $\gamma_c = 0.0005$. Other parameters as in Fig. 2.

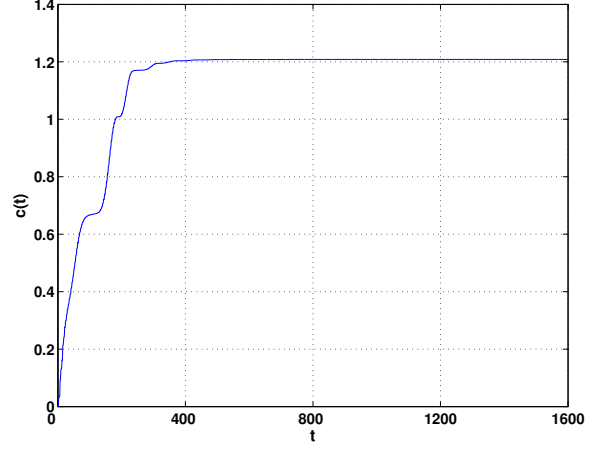


Figure 8. (Color online) Coupling coefficient $c(t)$ vs time t for 10-nodes coupled in a unidirectional ring. Adaptation algorithm according to Eq. (6). $\gamma = 0.015$, $\gamma_c = 0.0005$. Other parameters as in Fig. 2.

a ring with 2 nodes ($a_{jj} = 0$):

$$\begin{aligned}
 \dot{x}_j &= -y_j - z_j - K_j[x_j(t) - x_j(t - \tau)] \\
 &\quad + c(t)[x_{(k+1) \bmod 2}(t - \tau) - x_j(t)] \\
 \dot{y}_j &= x_j + ay_j \\
 \dot{z}_j &= b + z_j(x_j - \mu) \\
 \dot{K}_j &= \gamma(x_j(t) - x_j(t - \tau))[x_j(t) - 2x_j(t - \tau) \\
 &\quad + x_j(t - 2\tau)], \quad j = 1, \dots, N \\
 \dot{c}(t) &= \gamma_c(x_1(t) - x_2(t - \tau))[x_1(t) - 2x_2(t - \tau) \\
 &\quad + x_1(t - 2\tau)]
 \end{aligned} \tag{6}$$

It was found that for unidirectional rings this algorithm not only works for $N > 2$ but also for larger ring, e.g., of 5 or 10 nodes. It ensures the convergence of c to some appropriate value while all local coefficients K_i converge each to its own value stabilizing the unstable period-1 orbit in the local node. The adaptation process synchronizes the network with the appropriate accuracy.

The simulation results for 10 nodes are shown in .. 7-9: Figure 7 and 8 show the time series for K_1, \dots, K_{10} and c , respectively. Figure 9 depicts the synchronization accuracy for $t \in [0, 800]$ (top) and $t \in [1500, 1580]$ (bottom), respectively. From the small synchronization error for $t > 1500$ we conclude that synchronization is achieved.

2.5 Modification of the adaptation algorithm to improve synchronization

As shown in the previous Section, the final values of the self-feedback coefficients K_1, \dots, K_N differ due to the different initial states of the nodes. As already discussed, this leads to a non-vanishing synchronization error in the case that τ is not perfectly equal to the period of the stabilized orbit, which is usually the

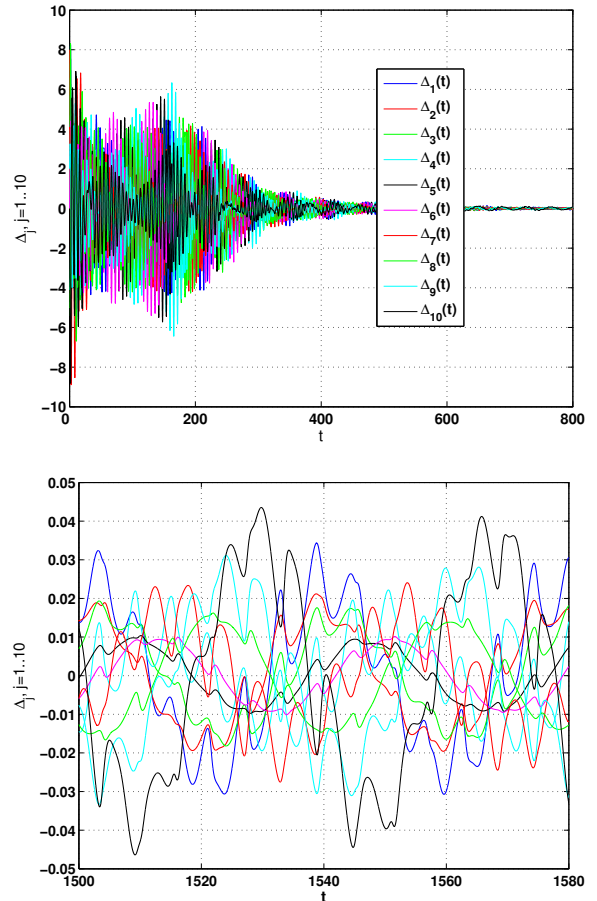


Figure 9. (Color online) Differences $\Delta_j = y_{j+1} - y_j$, $j = 1, \dots, 9$, $\Delta_{10} = y_1 - y_{10}$ (top) and their final values (bottom) vs time t for 10-nodes coupled in a unidirectional ring. Adaptation algorithm according to Eq. (6). $\gamma = 0.015$, $\gamma_c = 0.0005$. Other parameters as in Fig. 2.

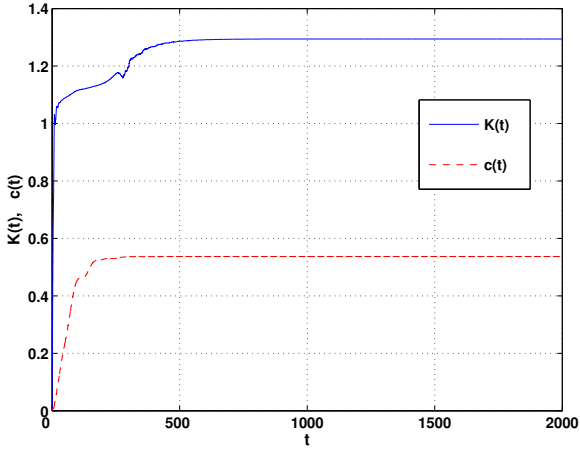


Figure 10. (Color online) Common self-feedback coefficient $K(t)$ and coupling coefficient $c(t)$ vs t for 5-nodes coupled in a unidirectional ring. Adaptation according to Eq. (7). $\gamma = 0.05$, $\gamma_c = 0.0005$. Other parameters as in Fig. 2.

case in experimental situations and even in numerical simulations.

The synchronization error can be decreased if all self-feedback coefficients K_1, \dots, K_N are chosen equal and are adapted at the same rate, i.e., $K_1(t), \dots, K_N(t) = K(t)$. The local adaptation algorithm of each K_i , as discussed in Section 2.3, is based only on the state variable x_i . The main idea of the modification proposed here is to use the arithmetic mean of the right-hand side of Eq. (5). Then, the SG-algorithm for a network of N nodes reads:

$$\begin{aligned} \dot{x}_j &= -y_j - z_j - K(t)[x_j(t) - x_j(t - \tau)] + \\ &\quad + c(t) \sum_{k=1}^N a_{jk} [x_k(t - \tau) - x_j(t)] \\ \dot{y}_j &= x_j + ay_j \\ \dot{z}_j &= b + z_j(x_j - \mu) \\ \dot{K}(t) &= \gamma \frac{1}{N} \sum_{j=1}^N (x_j(t) - x_j(t - \tau)) \cdot \\ &\quad \cdot [x_j(t) - 2x_j(t - \tau) + x_j(t - 2\tau)] \\ \dot{c}(t) &= \gamma_c (x_1(t) - x_2(t - \tau)) [x_1(t) - 2x_2(t - \tau) + \\ &\quad + x_1(t - 2\tau)] \end{aligned} \quad (7)$$

Our simulation results show that at least for 5 nodes coupled in a unidirectional ring almost perfect synchronization can be achieved: The time series of $K(t)$ and $c(t)$ are depicted in Fig. 10; the synchronization error is shown in Fig. 11. The final accuracy of synchronization is $\varepsilon_x = 2 \cdot 10^{-14}$, $\varepsilon_y = 2 \cdot 10^{-14}$, $\varepsilon_z = 5 \cdot 10^{-14}$ and therefore several order of magnitude smaller than in the case of adapting each of the K_i separately, as was done in Section 2.3.

Linear stability analysis For the system given by Eq. (7), we carry out a linear stability analysis which

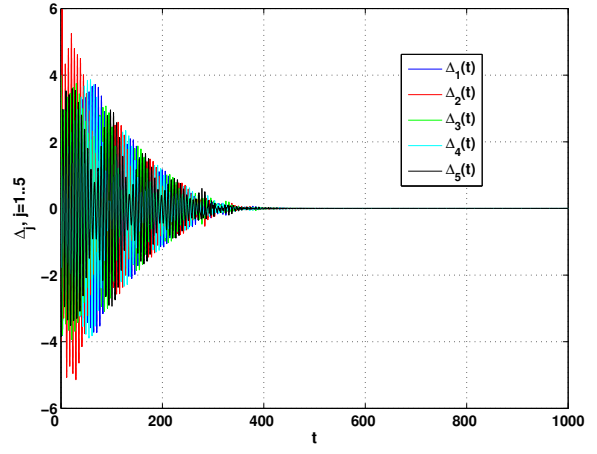


Figure 11. (Color online) Differences $\Delta_j^x = x_{j+1} - x_j$, $j = 0, \dots, 4$, $\Delta_5^x = x_1 - x_5$ vs time t for 5 nodes coupled in a unidirectional ring. Adaptation according to Eq. (7). $\gamma = 0.05$, $\gamma_c = 0.0005$. Other parameters as in Fig. 2.

can be used to predict to which values K and c should converge for successful synchronization in the periodic state. The synchronized and periodic solution $\mathbf{X}_s \equiv (x_s, y_s, z_s, K_s, c_s)$ of Eq. (7) is given by:

$$\begin{aligned} \dot{x}_s(t) &= -y_s(t) - z_s(t) \\ \dot{y}_s(t) &= x_s(t) + ay_s(t) \\ \dot{z}_s(t) &= b + z_s(t)[x_s(t) - \mu] \\ \dot{K}_s &= 0 \\ \dot{c}_s &= 0. \end{aligned} \quad (8)$$

Thus, K_s and c_s are just constants. We linearize Eq. (7) around this solution to obtain a variational equation:

$$\dot{\xi} = \mathbb{1}_N \otimes [D\mathbf{f}(\mathbf{X}_s(t))\xi + K_s \mathbf{H}\xi_\tau] + c_s \mathbf{A} \otimes \mathbf{H}\xi_\tau \quad (9a)$$

$$\dot{\delta K} = 0 \quad (9b)$$

$$\dot{\delta c} = 0, \quad (9c)$$

where $\xi = (x_1 - x_s, y_1 - y_s, y_1 - y_s, \dots, x_N - x_s, y_N - y_s, y_N - y_s)$, $\delta K = K - K_s$ and $\delta c = c - c_s$. The Jacobian matrix $D\mathbf{f}(\mathbf{X}_s(t))$ is given by:

$$D\mathbf{f}(\mathbf{X}_s(t)) = \begin{pmatrix} -(K_s + c_s) - 1 & -1 & \\ 1 & a & 0 \\ z_s & 0 & x_s - \mu \end{pmatrix} \quad (10)$$

\mathbf{H} describes the coupling scheme of the three variables x, y, z , which is identical for cross-coupling and self-coupling:

$$\mathbf{H} = \begin{pmatrix} 1 & 0 & 0 \\ 0 & 0 & 0 \\ 0 & 0 & 0 \end{pmatrix} \quad (11)$$

Eq. (9a) can be blockdiagonalized to obtain a Master stability equation [Pecora and Carroll, 1998].

$$\dot{\delta\mathbf{X}} = Df(\mathbf{X}_s(t))\delta\mathbf{X} + (K_s + c_s\nu_k)\mathbf{H}\delta\mathbf{X}_\tau \quad (12a)$$

$$\dot{\delta K} = 0 \quad (12b)$$

$$\dot{\delta c} = 0 \quad (12c)$$

where $\delta\mathbf{X} \in \mathbb{R}^3$ describes the deviation from the synchronized state in the eigensystem of \mathbf{A} , and ν_k are the eigenvalues of \mathbf{A} . Thus in the case of a unidirectional ring: $\nu_k = e^{\frac{2\pi i}{N}k}$ with $k = 1, \dots, N$. From Eq. (12a) the largest Lyapunov exponent $\Lambda(\nu_k)$ can be calculated numerically for all $k = 1, \dots, N$. $\nu_0 \equiv \nu_N$ is called the longitudinal eigenvalue since it describes deviations longitudinal to the synchronized orbit. Thus, its value is determined by the type of the synchronized dynamics: If the synchronized orbit is periodic, then $\Lambda(\nu_0) = 0$ holds, whereas for chaos synchronization the longitudinal Lyapunov exponent is positive: $\Lambda(\nu_0) > 0$. All other eigenvalues ν_k describe deviations transversal to the synchronization manifold. Hence, for stable synchronization $\Lambda(\nu_k) < 0$, $k = 1, \dots, N - 1$, must hold. From Eq. (12a) we calculate $\Lambda(\nu_0)$ (Fig. 12 (top)) and $\max_k \Lambda(\nu_k)$ (Fig. 12 (bottom)). In Fig. 12 (top) all values with $|\Lambda(\nu_0)| < 0.002$ are approximately set to 0 and colored in black. Hence, the black region in Fig. 12 (top) indicates periodic behavior in the synchronization manifold. The blue region in Fig. 12 (bottom) indicates that the largest longitudinal Lyapunov exponent is negative, i.e., the synchronization is stable. The red full circle marks the final values of K and c reached in the adaptive simulation presented in Fig. 10. The location of this circle inside the black region (top panel) and the blue region (bottom panel) confirms that stabilization of a periodic orbit and synchronization are achieved simultaneously. Note that Equations (12b) and (12c) describe the shift invariance of the system along the K and c axis. Therefore, the additional Lyapunov exponents, which arise if we consider Eqs. (12a)-(12c) instead of only Eq. (12a) are equal to zero and are not decisive for stability.

3 SG adaptation algorithm for noisy measurements

In experiments and engineering applications, the exact state of a system is usually unknown. In this Section We present a modification of our algorithm for applications in noisy environments. As in Section 2.5, we consider a network of N nodes coupled in a unidirectional ring with simultaneous adaptation of K and c . However, we assume that for the adaptation algorithms the exact values of the x -coordinates are unknown, i.e., we have only noisy measurements $h_i(t) =$

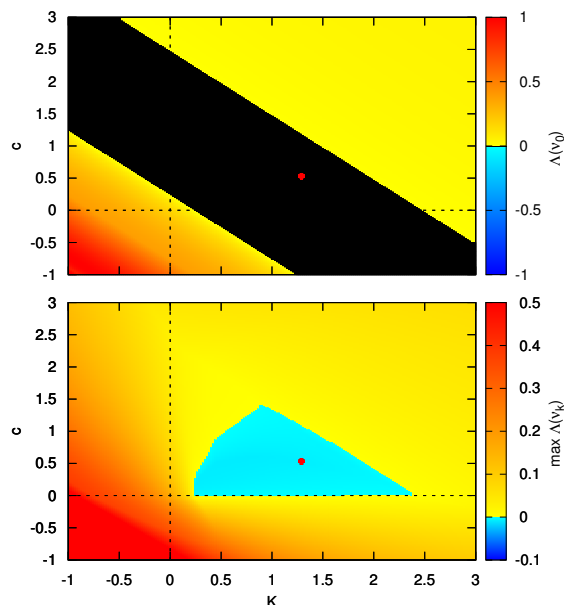


Figure 12. (Color online) Density plot of the stability regime in the (K, c) parameter space: The Master stability function evaluated at the longitudinal (top) and the dominant transversal (bottom) eigenvalue of the coupling matrix is plotted for the Rössler system: $\Lambda(\nu_0) > 0$ (top) and $\max \Lambda(\nu_k)$ (bottom) calculated from Eq. (12a). System parameters as in Fig. 2. The red full circle marks the final values of K and c which are reached by the adaptive simulation presented in Fig. 10.

$x_i(t) + D\xi_i(t)$, $i = 1, \dots, N$ of the variables $x_i(t)$:

$$\begin{aligned} \dot{x}_j &= -y_j - z_j - K(t)[x_j(t) - x_j(t - \tau)] \\ &\quad + c(t)[x_{(j+1) \bmod N}(t - \tau) - x_j(t)] \\ \dot{K}(t) &= \gamma \frac{1}{N} \sum_{j=1}^N (h_j(t) - h_j(t - \tau)) [h_j(t) - \\ &\quad - 2h_j(t - \tau) + h_j(t - 2\tau)] \\ \dot{c}(t) &= \gamma_c (h_1(t) - h_2(t - \tau)) [h_1(t) - \\ &\quad - 2h_2(t - \tau) + h_1(t - 2\tau)], \end{aligned} \quad (13)$$

where $\xi(t)$ is Gaussian white noise with zero mean and unity variance. The noise intensity is defined by the parameter D .

The standard way to overcome the effect of noise in the application of the SG-method is to introduce an inner deadzone in the adaptation algorithm [Fradkov, 1990; Fradkov, 2007]. This deadzone prevents the divergence of the adaptation algorithms when the exact values of the state variables are not available. The SG adaptation algorithm after the introduction of inner

dead zones is given by:

$$\begin{aligned} \dot{K}(t) &= \begin{cases} \tilde{u}_K(t) & \text{if } |\tilde{u}_K(t)| \geq \Delta_K, \\ 0 & \text{otherwise,} \end{cases} \\ \tilde{u}_K(t) &= \gamma \frac{1}{N} \sum_{j=1}^N (h_j(t) - h_j(t - \tau)) [h_j(t) - \\ &\quad - 2h_j(t - \tau) + h_j(t - 2\tau)] \\ \dot{c}(t) &= \begin{cases} \tilde{u}_c(t) & \text{if } |\tilde{u}_c(t)| \geq \Delta_c, \\ 0 & \text{otherwise,} \end{cases} \\ \tilde{u}_c(t) &= \gamma_c (h_1(t) - h_2(t - \tau)) [h_1(t) - \\ &\quad - 2h_2(t - \tau) + h_1(t - 2\tau)], \end{aligned} \quad (14)$$

where Δ_c and Δ_K define the dead zones.

This adaptation algorithm can stabilize at least 5 nodes coupled in a unidirectional ring for $D = 0.1$, $\Delta_K = 0.25$, $\Delta_c = 0.01$: In Fig. 13 the synchronization error is depicted for $t \in [0, 750]$ (top) and for $t \in [1450, 1500]$ (bottom). As can be seen in the bottom panel, the synchronization error for large t is of order of magnitude 10^{-3} . Figures 14 and 16 depict $\dot{K}(t)$ and $\dot{c}(t)$, respectively.

Figure 14 depicts $\dot{K}(t)$ for a non-zero dead zone in red and for a zero dead zone in blue. In the case of a non-zero dead zone and sufficiently large t , $K(t)$ is equal to zero, interrupted by a few peaks. This means that the control is successful and no further adaptation of K is needed. This can also be seen in Fig. 16 where the corresponding time series for K is depicted as a solid blue line. If no dead zone is introduced, $\dot{K}(t)$ does not vanish and is larger than zero. This means that K is constantly driven to large values out of the interval appropriate for control and the system quickly diverges. The same phenomenon can be observed in the adaptation of c : In Fig. 16 green lines mark the adaptation with and blue lines without a dead zone, respectively. The time series of c with a dead zone is shown in Fig. 16 as a dashed green line.

4 Conclusion

We have presented a method for self-adaptation of the self-feedback coefficients and coupling coefficients in the control of delay-coupled networks of chaotic Rössler oscillators. This method allows us to adaptively determine the coefficients such that locally a stabilization of a periodic orbit is achieved, while globally all nodes synchronize, i.e., after control becomes effective, the network is in a periodic zero-lag synchronized state. Our algorithm is based on the speed gradient method.

First, we have shown that for a fixed coupling coefficient c , an adaptation of the self-feedback coefficients K_1, \dots, K_N can be designed in such a way that the orbits are stabilized. This stabilization process is compatible with the synchronization process. As stabilization of the orbits is possible in an interval of values of

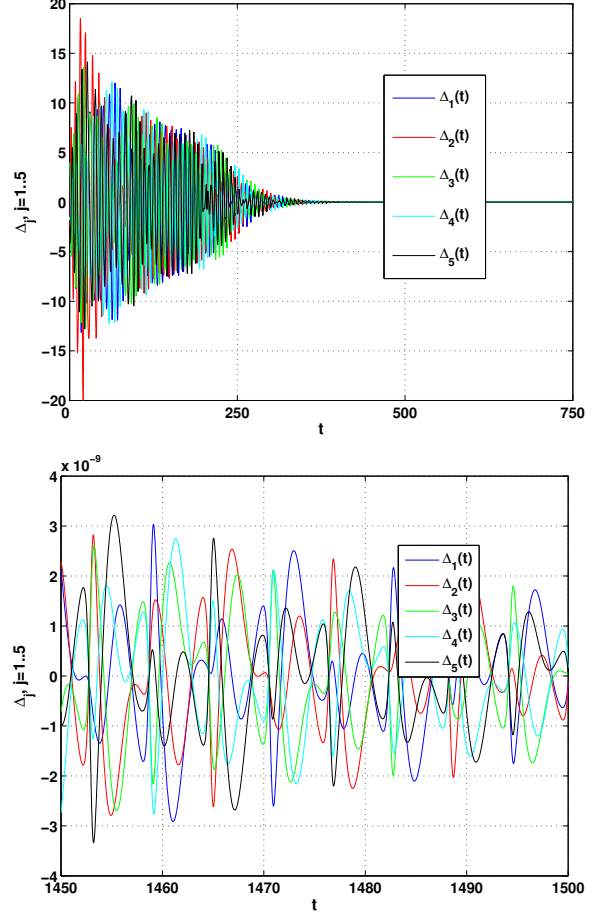


Figure 13. (Color online) Differences $\Delta_j^x = x_{j+1} - x_j$, $j = 1, \dots, 4$, $\Delta_5 = x_1 - x_5$ (top) and their final values (bottom) vs time t for noisy measurement with $D = 0.1$. Adaptation according to Eq. (14). $N = 5$, $\gamma = 0.02$, $\gamma_c = 0.0001$. Other parameters as in Fig. 2.

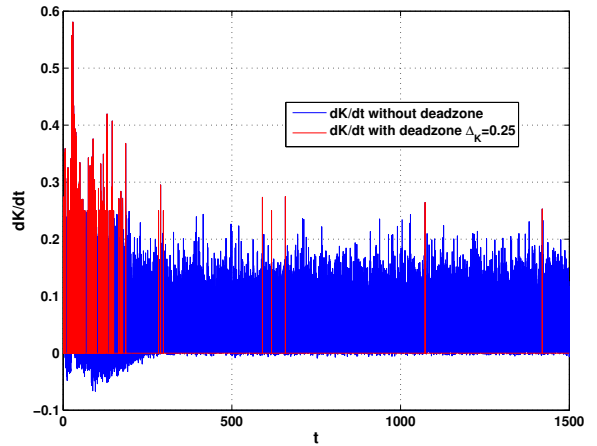


Figure 14. (Color online) \dot{K} without dead zone and with dead zone ($\Delta_K = 0.25$) vs t for noisy measurement with $D = 0.1$. Adaptation according to Eq. (14). $N = 5$, $\gamma = 0.02$, $\gamma_c = 0.0001$. Other parameters as in Fig. 2.

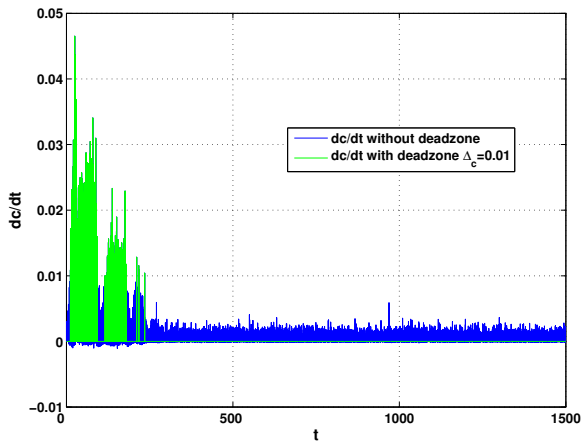


Figure 15. (Color online) \dot{c} without dead zone and with dead zone ($\Delta_c = 0.01$) vs t for noisy measurement with $D = 0.1$. Adaptation according to Eq. (14). $N = 5$, $\gamma = 0.02$, $\gamma_c = 0.0001$. Other parameters as in Fig. 2.

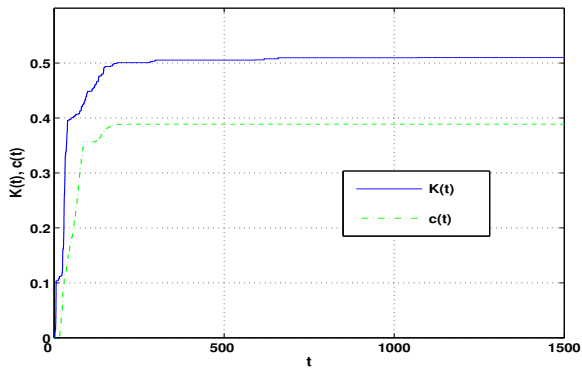


Figure 16. (Color online) Common self-feedback coefficient $K(t)$ and coupling coefficient $c(t)$ vs t for noisy measurement with $D = 0.1$. Adaptation according to Eq. (14). $N = 5$, $\gamma = 0.02$, $\gamma_c = 0.0001$. Other parameters as in Fig. 2.

K_i , and the initial conditions for all nodes in the network are different, the final values of the K_i differ. In the case that the delay time is not exactly equal to the period of the orbit, this leads to a non-vanishing synchronization error. In our simulations synchronization with an accuracy of less than 1% was achieved. The limitation of a non-vanishing synchronization error can be overcome if all nodes are controlled by the same self-feedback coefficient.

Further, we have demonstrated that in addition to the self-feedback coefficient the coupling coefficient c can be adapted as well. This enables synchronization of the network even in the case when an appropriate coupling strength is unknown.

In experimental and engineering applications the exact state of our systems is often unknown because measurements are affected by noise. To ensure the convergence of our method in the presence of noise we have introduced dead zones in the adaptation algorithm.

Chaos control and control of synchronization are of

great interest for a variety of systems in physics, biology, medicine and mechanical engineering. We believe that our method is a promising extension of the existing methods for controlling chaos and synchronization in networks. In particular, our method is useful in cases where parameters are unknown or drift as our method provides tools to find and track appropriate control parameters adaptively. The extension of our method to noisy measurement ensures the applicability to real world systems.

Acknowledgements

PG thanks the DAAD program "Mikhail Lomonosov (B)". JL and ES acknowledge support by Deutsche Forschungsgemeinschaft (DFG) in the framework of SFB 910. This work was also supported by the German-Russian Interdisciplinary Science Center (GRISC) via the German Academic Exchange Service (DAAD).

References

- Ahlborn, A. and Parlitz, U., Control and synchronization of spatiotemporal chaos, *Phys. Rev. E* **77**, 1, 016201 (2008).
- Baba, N. , Amann, A. , Scholl, E. and Just, W., Giant improvement of time-delayed feedback control by spatio-temporal filtering, *Phys. Rev. Lett.* **89**, 074101 (2002).
- Balanov, A. G. , Janson, N. B. and Schöll, E., Delayed feedback control of chaos: Bifurcation analysis, *Phys. Rev. E* **71**, 016222 (2005).
- Choe, C.-U., Dahms, T., Hövel, P. and Schöll, E. , Controlling synchrony by delay coupling in networks: from in-phase to splay and cluster states, *Phys. Rev. E* **81**, 2, 025205(R) (2010).
- Dahms, T., Lehnert, J. and Scholl, E. , Cluster and group synchronization in delay-coupled networks, *Phys. Rev. E* **86**, 1, 016202 (2012).
- Fradkov, A. L., Speed-gradient scheme and its application in adaptive control problems , *Autom. Remote Control* **40**, 1333 (1979).
- A. L. Fradkov, *Adaptive Control in Large-scale Systems*, (M.:Nauka, 1990, in Russian).
- Fradkov, A. L., Application of cybernetic methods in physics, *Physics-Usppekhi* **48**, 2, 103 (2005).
- A. L. Fradkov, *Cybernetical Physics: From Control of Chaos to Quantum Control* (Springer, 2007).
- Guzenko, P. Y., Hövel, P., Flunkert, V., Fradkov, A. L. and Schöll, E., Adaptive Tuning of Feedback Gain in Time-Delayed Feedback Control, *Proc. 6th EUROMECH Nonlinear Dynamics Conference (ENOC-2008)*, ed. A. Fradkov, B. Andrievsky, IPACS Open Access Library <http://lib.physcon.ru> , (2008).
- Just, W. , Bernard, T. , Ostheimer, M. , Reibold, E. and Benner, H. , Mechanism of time-delayed feedback control, *Phys. Rev. Lett.* **78**, 203 (1997).
- Just, W. , Fiedler, B. , Flunkert, V., Georgi, M. , Hövel, P. and Schöll, E., Beyond odd number limitation: a

- bifurcation analysis of time-delayed feedback control, *Phys. Rev. E* **76**, 026210 (2007).
- Kehrt, M., Hövel, P., Flunkert, V., Dahlem, M. A., Rodin, P. and Schöll, E., Stabilization of complex spatio-temporal dynamics near a subcritical Hopf bifurcation by time-delayed feedback, *Eur. Phys. J. B* **68**, 557 (2009).
- Kim, M., Bertram, M., Pollmann, M., von Oertzen, A., Mikhailov, A. S., Rotermund, H. H. and Ertl, G., Controlling chemical turbulence by global delayed feedback: Pattern formation in catalytic CO oxidation on Pt(110), *Science* **292**, 1357 (2001).
- Kyrychko, Y. N., Blyuss, K. B., Hogan, S. J. and Schöll, E., Control of spatio-temporal patterns in the Gray-Scott model, *Chaos* **19**, 4, 043126 (2009).
- Lehnert, J., Hövel, P., Flunkert, V., Guzenko, P.Y., Fradkov, A. L. and Schöll, E., Adaptive tuning of feedback gain in time-delayed feedback control, *Chaos* **21**, 043111 (2011)
- Pecora, L. M. and Carroll, T. L. Master stability function for Synchronized Coupled Systems, *Phys. Rev. Lett.*, (1998)
- Pikovsky, A.S., Rosenblum, M.G. and Kurths, J., Synchronization, A Universal Concept in Nonlinear Sciences, Cambridge University Press, (2001).
- Postlethwaite, C. M. and Silber, M., Stabilizing unstable periodic orbits in the Lorenz equations using time-delayed feedback control, *Phys. Rev. E* **76**, 5, 056214 (2007).
- Pyragas, K., Continuous control of chaos by self-controlling feedback, *Phys. Lett. A* **170**, 421 (1992).
- Pyragas, K., Delayed feedback control of chaos, *Phil. Trans. R. Soc. A* **364**, 1846, 2309 (2006).
- Selivanov, A. A., Lehnert, J., Dahms, T., Hövel, P., Fradkov, A. L. and Schöll, E., Adaptive synchronization in delay-coupled networks of Stuart-Landau oscillators, *Phys. Rev. E* **85**, 016201 (2012).
- Schlesner, J., Amann, A. Janson, N. B., Just, W. and Schöll, E., Self-stabilization of high frequency oscillations in semiconductor superlattices by time-delay autosynchronization, *Phys. Rev. E* **68**, 066208 (2003).
- Handbook of Chaos Control*, edited by E. Schöll and H. G. Schuster (Wiley-VCH, Weinheim, 2007), second completely revised and enlarged edition.
- Schöll, E., Selivanov, A. A., Lehnert, J., Dahms, T., Hövel, P. and Fradkov, A. L., Control of synchronization in delay-coupled networks, *Int. J. Mod. Phys. B* **26**, 25, 1246007 (2012)